Available online at www.sciencedirect.com
ScienceDirect
Journal of Organometallic Chemistry 693 (2008) 269–277
Journal of Organometallic Chemistry
www.elsevier.com/locate/jorganchem

Reactions of Mo(II)-tetraphosphine complex $[MoCl_2\{meso\text{-}o\text{-}C_6H_4(PPhCH_2CH_2PPh_2)_2\}]$ with a series of small molecules

Takeshi Ohnishi, Hiroko Tsuboi, Hidetake Seino, Yasushi Mizobe *

Institute of Industrial Science, The University of Tokyo, Komaba, Meguro-ku, Tokyo 153-8505, Japan

Received 26 June 2007; received in revised form 23 October 2007; accepted 30 October 2007
Available online 7 November 2007

Abstract

Reactions of Mo(II)-tetraphosphine complex $[MoCl_2(\kappa^4\text{-}\mathbf{P4})]$ (**2**; **P4** = *meso*-*o*-$C_6H_4(PPhCH_2CH_2PPh_2)_2$) with a series of small molecules have been investigated. Thus, treatment of **2** with alkynes RC≡CR′ (R = Ph, R′ = H; R = *p*-tolyl, R′ = H; R = Me, R′ = Ph) in benzene or toluene gave neutral mono(alkyne) complexes $[MoCl_2(RC{\equiv}CR')(\kappa^3\text{-}\mathbf{P4})]$ containing tridentate **P4** ligand, which were converted to cationic complexes $[MoCl(RC{\equiv}CR')(\kappa^4\text{-}\mathbf{P4})]Cl$ having tetradentate **P4** ligand upon dissolution into $CDCl_3$ or CD_2Cl_2. The latter complexes were available directly from the reactions of **2** with the alkynes in CH_2Cl_2. On the other hand, treatment of **2** with 1 equiv. of XyNC (Xy = 2,6-$Me_2C_6H_3$) afforded a seven-coordinate mono(isocyanide) complex $[MoCl_2(XyNC)(\kappa^4\text{-}\mathbf{P4})]$ (**7**), which reacted further with XyNC to give a cationic bis(isocyanide) complex $[MoCl(XyNC)_2(\kappa^4\text{-}\mathbf{P4})]Cl$ (**8**). From the reaction of **2** with CO, a mono(carbonyl) complex $[MoCl_2(CO)(\kappa^4\text{-}\mathbf{P4})]$ (**9**) was obtained as a sole isolable product. Reaction of **9** with XyNC afforded $[MoCl(CO)(XyNC)(\kappa^4\text{-}\mathbf{P4})]Cl$ (**10a**) having a pentagonal–bipyramidal geometry with axial CO and XyNC ligands, whereas that of **7** with CO resulted in the formation of a mixture of **10a** and its isomer **10b** containing axial CO and Cl ligands. Structures of **7** and **9** as well as $[MoCl(XyNC)_2(\kappa^4\text{-}\mathbf{P4})][PF_6]$(**8′**) and $[MoCl(CO)(XyNC)(\kappa^4\text{-}\mathbf{P4})][PF_6]$ (**10a′**) derived by the anion metathesis from **8** and **10a**, respectively, were determined in detail by the X-ray crystallography.

Keywords: Mo complex; Tetraphosphine; Alkyne; Isocyanide; CO

1. Introduction

We found previously the unexpected formation of the tetraphosphine complexes $[M(\kappa^4\text{-}\mathbf{P4})(dppe)]$ (**1**; M = Mo, W; **P4** = *meso*-*o*-$C_6H_4(PPhCH_2CH_2PPh_2)_2$, dppe = $Ph_2PCH_2CH_2PPh_2$) by heating the solutions of *trans*-$[M(N_2)_2(dppe)_2]$ in the presence of 1 equiv. of dppe, where the unprecedent tetraphosphine **P4** forms through the condensation of two dppe ligands in the coordination sphere of Mo or W [1]. Subsequent studies on the reactivities toward a series of small molecules have disclosed that **1** (M = Mo) can undergo not only the substitutions of bound P atoms by one, two, or three molecules such as nitrile, CO, and isocyanide [2] but also the C=O and C=S bond cleaving reactions of CO_2 and RNCS, respectively [3]. Interesting feature observed for **P4** in these reactions is its ability to change the coordination mode readily from κ^4 to κ^3, and even to κ^2.

More recently we have isolated the dihalide complexes $[MX_2(\kappa^4\text{-}\mathbf{P4})]$ (M = Mo: X = Cl (**2**), Br; M = W: X = Br) by treatment of **1** with $PhCH_2X$, which are the diamagnetic complexes having a trigonal–prismatic structure shown in Eq. (1) with 16-electron, coordinatively unsaturated metal centers [4]. As for the reactivities of **2**, we have reported already the reactions with diazoalkanes in a preliminary form, which include the catalytic conversion of $N_2CHCOOEt$ into EtOCOCH=CHCOOEt as well as the formation of the diazoalkane complexes such as

* Corresponding author. Fax: +81 3 5452 6361.
E-mail address: ymizobe@iis.u-tokyo.ac.jp (Y. Mizobe).

0022-328X/$ - see front matter © 2007 Elsevier B.V. All rights reserved.
doi:10.1016/j.jorganchem.2007.10.054

$[MoCl_2(NN=CHSiMe_3)(\kappa^3\text{-}\mathbf{P4})]$ and $[MoCl(NN=CHSiMe_3)(\kappa^4\text{-}\mathbf{P4})][PF_6]$ [4]. Quite recently, it has also been demonstrated that **2** facilitates the N–N bond cleavage of organohydrazines to give nitrido and imido complexes $[MoCl(N)(\kappa^4\text{-}\mathbf{P4})]$ and $[MoCl(NR)(\kappa^4\text{-}\mathbf{P4})][PF_6]$ (R = Me, Ph). From the former nitrido complex, acylimido complexes of two types $[MoCl_2(NCOMe)(\kappa^3\text{-}\mathbf{P4})]$ (**3a**) and $[MoCl(NCOMe)(\kappa^4\text{-}\mathbf{P4})][PF_6]$ (**3b**) have been derivatized by treatment with MeCOCl and fully characterized by X-ray diffraction [5]. In this paper, we wish to describe the details of the reactions of **2** with other selected small molecules, forming a series of new **P4** complexes

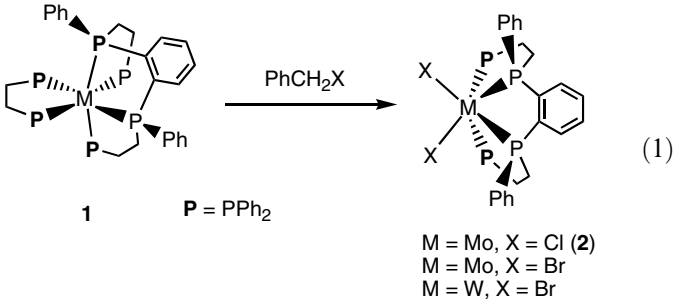

(1)

2. Results and discussion

2.1. Reactions of 2 with alkynes

When reacted with PhC≡CH in benzene at room temperature, **2** was converted into a neutral mono(alkyne) complex $[MoCl_2(PhC{\equiv}CH)(\kappa^3\text{-}\mathbf{P4})]$ (**4a**), which was isolated as a green solid in moderate yield (Scheme 1). The $^{31}P\{^1H\}$ NMR spectrum of a C_6D_6 solution shows four signals including one high-field doublet at δ −10.4, which is characteristic of the free P atom of **P4**. This spectral feature is in good agreement with that of the crystallographically characterized **3a** [5], suggesting that **4a** also has the octahedral geometry with the κ^3-**P4** ligand as observed for **3a**. By the donation of 4 electrons from the side-on bound alkyne, 18-electron count of the Mo center may be satisfied by this six-coordinate, octahedral geometry. In the ^1H NMR spectrum, the alkynic proton resonates at δ 11.4 as the doublet of doublets of doublets.

Interestingly, upon dissolution into $CDCl_3$, **4a** is readily transformed into a cationic mono(alkyne) complex $[MoCl(PhC{\equiv}CH)(\kappa^4\text{-}\mathbf{P4})]Cl$ (**4b**), as indicated by the $^{31}P\{^1H\}$ NMR spectrum exhibiting only two signals comparable to that of the X-ray analyzed **3b** [5]. The alkynic proton appears in the ^1H NMR spectrum at δ 12.4 as the triplet of triplets. As expected, the reaction of **2** with PhC≡CH conducted in CH_2Cl_2 also gave **4b** as a green solid in moderate yield upon precipitation from CH_2Cl_2-hexane. When **4b** was redissolved in C_6D_6, the NMR spectra coincide with those of **4a**, indicating that the structures of **4** change reversibly, depending upon the polarity of the solvents. The structure proposed for **4b** on the basis of the X-ray structure of **3b** is shown in Scheme 1. This is supported quite recently by the X-ray analysis of the alkyne complex $[MoI(MeC{\equiv}CCOOMe)(\kappa^4\text{-}\mathbf{P4})]I$ derived by oxidizing the Mo(0) mono(alkyne) complex $[Mo(MeC{\equiv}CCOOMe)(\kappa^4\text{-}\mathbf{P4})]$ with I_2, which will be reported separately elsewhere [6]. It is also to be noted that the analogous structure was previously disclosed for the related diphosphine complexes *trans*-$[MoF(PhC{\equiv}CH)(dppe)_2][BF_4]$ [7] and *trans*-$[MoF(MeNHC{\equiv}CNHMe)(dppe)_2][BF_4]$ [8].

Reactions of **2** with TolC≡CH (Tol = *p*-tolyl) took place similarly at room temperature to give the corresponding $[MoCl_2(TolC{\equiv}CH)(\kappa^3\text{-}\mathbf{P4})]$ (**5a**) and $[MoCl(TolC{\equiv}CH)(\kappa^4\text{-}\mathbf{P4})]Cl$ (**5b**), although the reaction to prepare the former proceeded more cleanly when conducted in toluene at 60 °C. The inner alkyne MeC≡CPh also reacted with **2** at 60 °C in toluene or at room temperature in CH_2Cl_2, yielding $[MoCl_2(MeC{\equiv}CPh)(\kappa^3\text{-}\mathbf{P4})]$ (**6a**) and $[MoCl(MeC{\equiv}CPh)(\kappa^4\text{-}\mathbf{P4})]Cl$ (**6b**), respectively. On the other hand, from the reactions with alkynes such as RC≡CH (R = MeOCO, *n*-Bu, *t*-Bu) and PhC≡CPh, formations of the alkyne-containing complexes were inferred spectroscopically but the isolation of analytically pure products was unsuccessful.

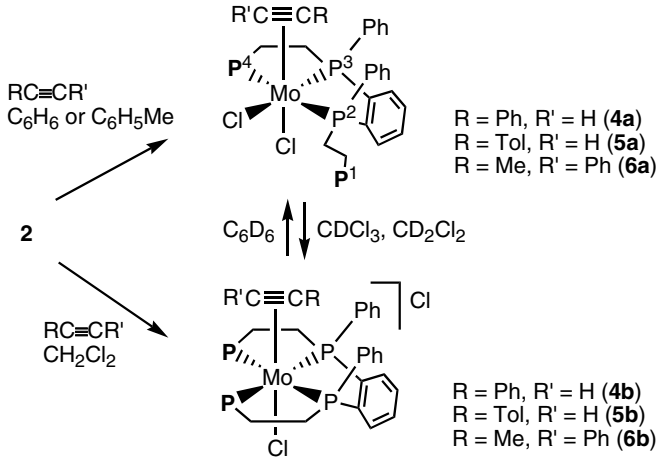

Scheme 1.

2.2. Reactions of 2 with isocyanide and CO

Reaction of **2** with 1 equiv. of XyNC (Xy = 2,6-$Me_2C_6H_3$) in toluene proceeded smoothly at room temperature to give a mono(isocyanide) complex $[MoCl_2(XyNC)(\kappa^4\text{-}\mathbf{P4})]$ (**7**) in moderate yield (Scheme 2). The X-ray analysis has disclosed the structure of **7** in detail, whose ORTEP drawing is depicted in Fig. 1 and selected bond distances and angles are listed in Table 1.

In contrast to the acylimido and alkyne complexes **3**–**6**, the isocyanide complex **7** is a seven-coordinate complex having a distorted monocapped octahedral geometry with P(3) as a capping atom on the P(2)–P(4)–C(47) face of the octahedron. Alternatively, it might also be possible to regard this structure as a monocapped trigonal–prism

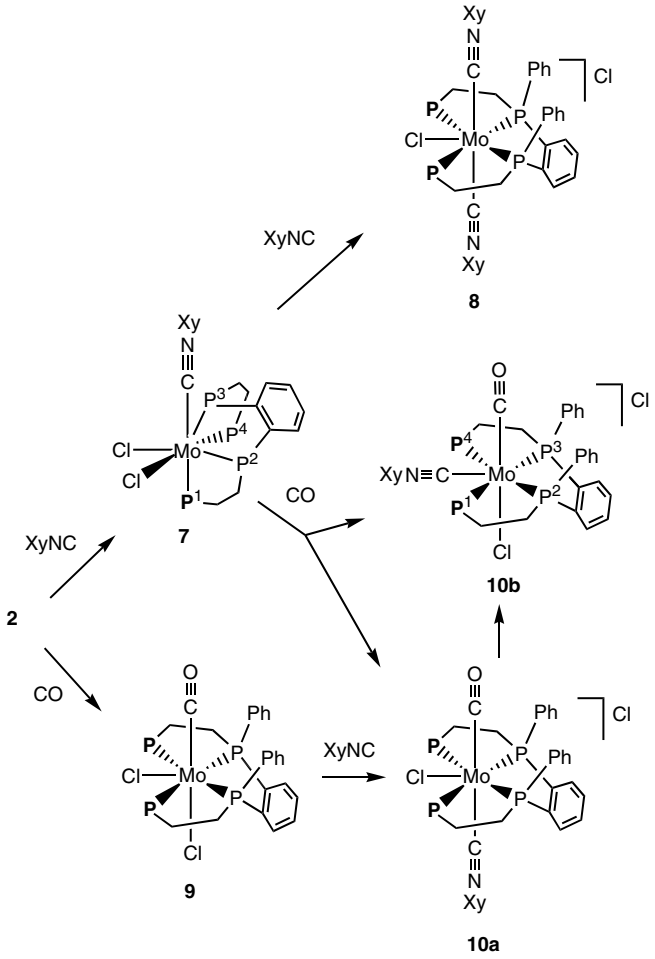

Scheme 2.

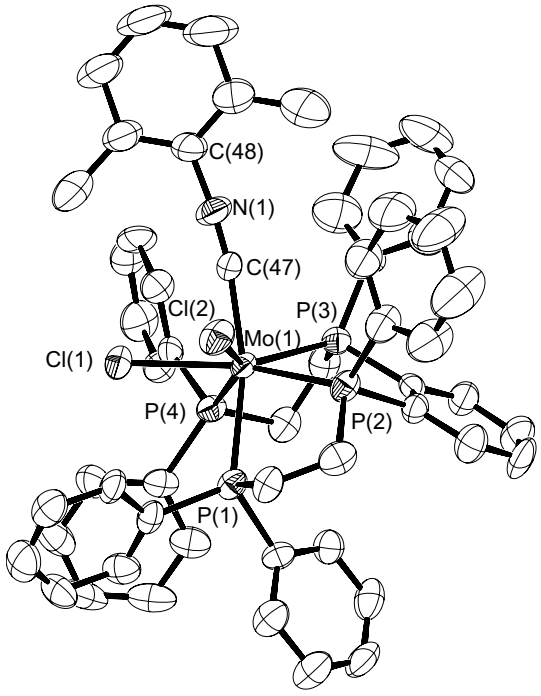

Fig. 1. An ORTEP drawing for **7** at 30% probability level. All hydrogen atoms are omitted for clarity.

Table 1
Selected bond distances (Å) and angles (°) in **7**

(a) Bond distance			
Mo–Cl(1)	2.535(2)	Mo–Cl(2)	2.558(2)
Mo–P(1)	2.556(2)	Mo–P(2)	2.470(2)
Mo–P(3)	2.441(2)	Mo–P(4)	2.511(2)
Mo–C(47)	2.036(9)	C(47)–N	1.16(1)
N–C(48)	1.39(1)		
(b) Bond angle			
P(1)–Mo–P(2)	75.07(8)	P(1)–Mo–P(3)	117.52(8)
P(1)–Mo–P(4)	87.00(7)	P(1)–Mo–Cl(1)	87.05(7)
P(1)–Mo–Cl(2)	82.97(8)	P(1)–Mo–C(47)	158.9(2)
P(2)–Mo–P(3)	73.37(8)	P(2)–Mo–P(4)	129.34(8)
P(2)–Mo–Cl(1)	149.31(8)	P(2)–Mo–Cl(2)	73.17(7)
P(2)–Mo–C(47)	108.0(2)	P(3)–Mo–P(4)	74.13(7)
P(3)–Mo–Cl(1)	137.30(8)	P(3)–Mo–Cl(2)	133.75(7)
P(3)–Mo–C(47)	82.8(2)	P(4)–Mo–Cl(1)	72.95(7)
P(4)–Mo–Cl(2)	151.69(8)	P(4)–Mo–C(47)	105.2(2)
Cl(1)–Mo–Cl(2)	80.13(7)	Cl(1)–Mo–C(47)	80.4(2)
Cl(2)–Mo–C(47)	78.2(2)	Mo–C(47)–N	169.7(7)
C(47)–N–C(48)	171.4(8)		

consisting of the P(2)–P(1)–Cl(2) and P(3)–P(4)–C(47) basal planes with the Cl(1) atom capping to the Cl(2)–P(1)–P(4)–C(47) rectangle. The XyNC molecule is bound to the Mo center in an linear end-on fashion with the Mo–C(47)–N(1) and C(47)–N(1)–C(48) angles of 169.7(7) and 171.4(8)°, respectively. The Mo–C(47) and C(47)–N(1) bond lengths are 2.036(9) and 1.16(1) Å, and the IR spectrum of **7** shows the ν(N≡C) band at 2026 cm^{-1}. For comparison, the octahedral Mo(0) complex [Mo(XyNC)(κ^3-**P4**)(dppe)], having the averaged Mo–C and C–N bond lengths in the Mo–C–N array at 2.00(1) and 1.20(2) Å, exhibits the ν(N≡C) band at 1848 cm^{-1} [2]. These data are consistent with the stronger electron-donating ability of the zero-valent Mo center to the XyNC ligand in the latter complex than the Mo(II) center in **7**. In the $^{31}P\{^1H\}$ NMR spectra of the $CDCl_3$ and C_6D_6 solutions, four signals with same intensities were observed, which is in agreement with the solid state structure containing four inequivalent P atoms. Based on the previous findings [1–5], two signals in the lower field are assignable unambiguously to the inner P atoms P^2 and P^3, while those in the higher field to the outer P atoms P^1 and P^4. However, further assignments of either P^2 or P^3 and either P^1 or P^4 were done tentatively as shown in Section 3, where the P atoms P^2 and P^1 having the longer Mo–P bonds in each pair were assigned to the resonances observed in the higher field.

Treatment of **2** with 3 equiv. of XyNC in toluene at room temperature for 1 h resulted in the precipitation of [MoCl(XyNC)$_2$(κ^4-**P4**)]Cl (**8**) from the reaction mixture as a red solid (Scheme 2). As expected, this cationic complex is highly soluble in polar CH_2Cl_2 and was able to be purified by crystallization from CH_2Cl_2-ether. This reaction proceeded more smoothly when conducted directly in CH_2Cl_2. The X-ray analysis was carried out to determine the structure by using the single crystal of [MoCl(XyNC)$_2$(κ^4-**P4**)][PF_6] (**8′**) obtained from **8** after the anion metathesis, which has disclosed the distorted pentagonal–

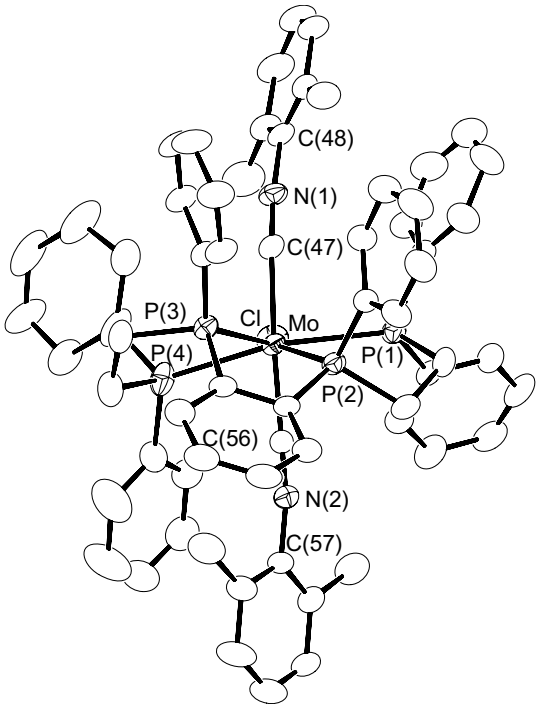

Fig. 2. An ORTEP drawing for the cation of **8′** at 30% probability level. All hydrogen atoms are omitted for clarity.

Table 2
Selected bond distances (Å) and angles (°) in **8′**

(a) Bond distance			
Mo–Cl	2.526(2)	Mo–P(1)	2.615(2)
Mo–P(2)	2.461(2)	Mo–P(3)	2.487(1)
Mo–P(4)	2.573(2)	Mo–C(47)	2.097(5)
Mo–C(56)	2.071(5)	C(47)–N(1)	1.171(6)
N(1)–C(48)	1.424(7)	C(56)–N(2)	1.176(7)
N(2)–C(57)	1.400(7)		
(b) Bond angle			
Cl–Mo–P(1)	78.54(5)	Cl–Mo–P(2)	148.47(5)
Cl–Mo–P(3)	141.92(5)	Cl–Mo–P(4)	74.50(6)
Cl–Mo–C(47)	78.1(2)	Cl–Mo–C(56)	91.8(2)
P(1)–Mo–P(2)	71.77(5)	P(1)–Mo–P(3)	135.56(5)
P(1)–Mo–P(4)	150.39(5)	P(1)–Mo–C(47)	83.5(2)
P(1)–Mo–C(56)	91.5(2)	P(2)–Mo–P(3)	69.58(4)
P(2)–Mo–P(4)	130.88(6)	P(2)–Mo–C(47)	108.1(2)
P(2)–Mo–C(56)	78.8(2)	P(3)–Mo–P(4)	73.98(5)
P(3)–Mo–C(47)	88.4(1)	P(3)–Mo–C(56)	101.6(1)
P(4)–Mo–C(47)	102.5(2)	P(4)–Mo–C(56)	77.5(2)
C(47)–Mo–C(56)	169.5(2)	Mo–C(47)–N(1)	170.6(4)
C(47)–N(1)–C(48)	170.9(5)	Mo–C(56)–N(2)	178.9(4)
C(56)–N(2)–C(57)	169.2(5)		

bipyramidal structure of the cation as shown in Fig. 2 and Table 2. In the cation, four P atoms as well as the Cl ligand consist of the equatorial plane and two XyNC molecules occupy the remaining axial positions. In a solid state, four P atoms are all inequivalent by deviating upward and downward alternately from the ideal equatorial plane. Two axial positions are not equivalent because of the orientation of two Ph groups and the phenylene group attached to the inner P atoms of **P4** ligand. In **8′**, the metrical parameters associated with two axial XyNC ligands are almost comparable except for the larger deviation of the Mo–C(47)–N(1) angle at 170.6(4)° from the linearity than the Mo–C(56)–N(2) angle at 178.9(4)°.

On the other hand, the $^{31}P\{^{1}H\}$ NMR spectrum of **8** in $CDCl_3$ indicates the symmetrical structure containing the mutually equivalent inner P^2 and P^3 atoms as well as the equivalent outer P^1 and P^4 atoms. In solution, the two inner P atoms as well as the two outer P atoms each become equivalent by the fluxional motion of the chelating rings. The ^{1}H NMR and IR spectra are consistent with the X-ray structure disclosed for **8′**.

As for the reaction of **2** with an excess amount of CO, coordination of CO proceeded smoothly at room temperature in toluene or CH_2Cl_2, but only the mono(carbonyl) complex $[MoCl_2(CO)(\kappa^4\text{-}\mathbf{P4})]$ (**9**) was obtained as the isolable product presumably because of the relatively weak electron-donating ability of the Mo(II) center in **9** to the π-acidic CO ligand (Scheme 2). This presents a contrast with the reaction of the zero-valent Mo complex **1** with CO, affording readily a bis(carbonyl) complex *cis*-$[Mo(CO)_2(\kappa^4\text{-}\mathbf{P4})]$ in addition to a mono(carbonyl) species $[Mo(CO)(\kappa^3\text{-}\mathbf{P4})(dppe)]$ [2]. To determine the detailed structure, the X-ray analysis has been carried out also for **9**.

A single crystal of **9** contained three crystallographically independent molecules having essentially identical structures. The ORTEP drawing of one molecule is shown in Fig. 3, while the selected bond distances and angles are listed in Table 3. Complex **9** is a neutral, seven-coordinate complex with the distorted pentagonal–bipyramidal geometry, where the equatorial positions are occupied by four P atoms of **P4** and one Cl ligand. The CO molecule binds to one axial site opposite to the phenylene group of **P4** with

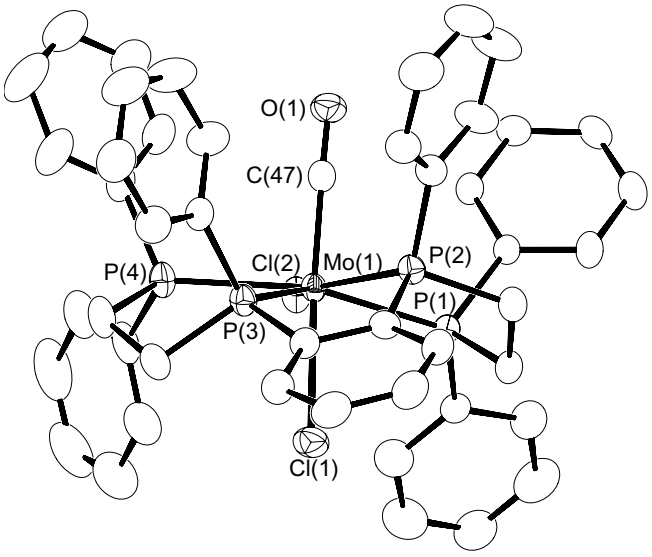

Fig. 3. An ORTEP drawing for the molecule 1 of **9** at 30% probability level. All hydrogen atoms are omitted for clarity.

Table 3
Selected bond distances (Å) and angles (°) in **9**

	Molecule 1	Molecule 2	Molecule 3
(a) Bond distance			
Mo–Cl(1)	2.640(1)	2.626(1)	2.612(1)
Mo–Cl(2)	2.541(1)	2.5228(9)	2.517(1)
Mo–P(1)	2.5514(8)	2.567(1)	2.558(1)
Mo–P(2)	2.492(1)	2.5133(8)	2.500(2)
Mo–P(3)	2.4859(9)	2.476(1)	2.471(1)
Mo–P(4)	2.5902(9)	2.590(1)	2.579(2)
Mo–C(47)	1.902(4)	1.887(4)	1.893(3)
C(47)–O(1)	1.162(6)	1.191(4)	1.178(4)
(b) Bond angle			
Cl(1)–Mo–Cl(2)	96.23(4)	89.97(3)	88.94(3)
Cl(1)–Mo–P(1)	78.88(3)	80.68(3)	78.78(3)
Cl(1)–Mo–P(2)	91.00(4)	91.12(3)	93.67(4)
Cl(1)–Mo–P(3)	76.71(3)	79.22(3)	78.17(3)
Cl(1)–Mo–P(4)	93.39(4)	94.73(3)	93.75(4)
Cl(1)–Mo–C(47)	175.8(1)	177.5(1)	178.6(1)
Cl(2)–Mo–P(1)	72.77(2)	72.95(3)	72.95(4)
Cl(2)–Mo–P(2)	144.59(3)	146.64(4)	146.70(3)
Cl(2)–Mo–P(3)	143.95(3)	143.15(3)	143.47(4)
Cl(2)–Mo–P(4)	74.19(3)	73.49(3)	74.36(3)
Cl(2)–Mo–C(47)	86.9(1)	91.4(1)	90.7(2)
P(1)–Mo–P(2)	74.75(3)	74.34(3)	75.03(4)
P(1)–Mo–P(3)	137.46(3)	137.82(3)	135.42(5)
P(1)–Mo–P(4)	144.92(3)	146.11(3)	146.55(4)
P(1)–Mo–C(47)	99.4(1)	97.7(1)	99.9(1)
P(2)–Mo–P(3)	71.42(3)	69.41(3)	68.99(4)
P(2)–Mo–P(4)	140.06(3)	139.53(4)	138.34(3)
P(2)–Mo–C(47)	84.8(1)	86.6(1)	85.9(2)
P(3)–Mo–P(4)	71.07(3)	72.47(3)	72.60(4)
P(3)–Mo–C(47)	102.37(1)	100.9(1)	102.8(1)
P(4)–Mo–C(47)	90.2(1)	87.7(1)	87.4(2)
Mo–C(47)–O(1)	178.2(2)	178.6(4)	178.3(4)

the angle of the C(axial)–Mo–Cl(axial) array at 175.8(1)–178.6(1)°.

The $^{31}P\{^{1}H\}$ NMR spectrum of **9** shows two signals with the same intensities, indicating that two inner P atoms and two outer P atoms of **P4** are each equivalent as observed for **8**. The IR spectrum exhibits the characteristic ν(C≡O) band at 1793 cm^{-1}. It is to be noted that the spectroscopic data indicate the formation of only one isomer for **9**, although coordination of CO to one equatorial position or the other axial site also seems possible.

The reaction of **9** with CO did not proceed further. However, treatment of **9** with XyNC in CH_2Cl_2 at room temperature afforded cleanly a carbonyl-isocyanide complex [MoCl(CO)(XyNC)(κ^4-**P4**)]Cl (**10a**) (Scheme 2). To determine the structure of **10a**, the X-ray diffraction has been carried out by using the single crystal of [MoCl(CO)(XyNC)(κ^4-**P4**)][PF_6] (**10a′**) obtained from **10a** after anion metathesis with KPF_6.

The single crystal of **10a′** contained two crystallographically independent molecules with essentially identical structures, and the view of the cation of one molecule is depicted in Fig. 4, while the selected bond distances and angles are summarized in Table 4. The cation has a distorted pentagonal–bipyramidal geometry with four P and one Cl atoms at the equatorial sites. The incorporated

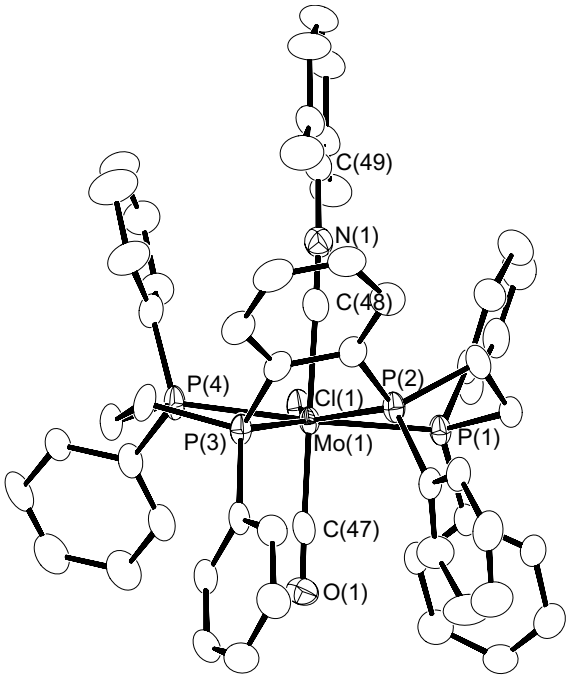

Fig. 4. An ORTEP drawing for the cation in the molecule 1 of **10a′** at 30% probability level. All hydrogen atoms are omitted for clarity.

XyNC is occupying the axial site *trans* to the CO ligand with the C–Mo–C angles of 175.0(2) and 172.6(2)° in two molecules. The Mo–C–O angles of 178.6(4) and 178.7(5)° as well as the Mo–C–N angles at 173.7(5) and 174.4(5)° indicate the common linear end-on coordination of both the CO and isocyanide molecules. Presumably due to the strong *trans* effect exerted by CO, replacement of the Cl ligand *trans* to CO in **9** proceeds selectively to give the product having the axial XyNC and CO ligands. From the $^{31}P\{^{1}H\}$ NMR data, the symmetrical structure in which the inner P atoms as well as the outer P atoms are each equivalent is indicated in a solution state. The ν(N≡C) and ν(C≡O) bands appear at 2089 and 1872 cm^{-1}, respectively, which are comparable to those at 2061 and 1861 cm^{-1}, observed for the X-ray analyzed, pentagonal–bipyramidal complex [MoH(PhNC)(CO)(dppe)$_2$][BF_4] having the PhNC and CO ligands at the axial positions [9].

In contrast, the reaction of the mono(isocyanide) complex **7** with CO in CH_2Cl_2 gave a mixture of two products. From the IR and NMR criteria, one product can be identified as **10a**, while the other product **10b** is presumed to be the isomer of **10a**, since these data for the other are well comparable to those of **10a**. The ratio of **10a** and **10b** in the reaction mixture is estimated to be 4:5 from the NMR spectra, which is unvariable after 24 h at room temperature. However, when the $ClCH_2CH_2Cl$ solution of this mixture was heated to the refluxing temperature for 2 h, it turned out that the resultant mixture contained only **10b**.

By converting **10b** obtained by this procedure to **10b′** through anion metathesis using KPF_6, some single crystals were available also for **10b′**. Although the X-ray analysis using these crystals did not complete satisfactorily because

Table 4
Selected bond distances (Å) and angles (°) in **10a′**

	Molecule 1	Molecule 2
(a) Bond distance		
Mo–Cl(1)	2.529(2)	2.527(2)
Mo–P(1)	2.576(1)	2.591(1)
Mo–P(2)	2.502(1)	2.467(2)
Mo–P(3)	2.507(2)	2..504(2)
Mo–P(4)	2.566(1)	2.558(1)
Mo–C(47)	1.972(6)	1.964(6)
Mo–C(48)	2.115(6)	2.108(5)
C(47)–O(1)	1.166(7)	1.169(7)
C(48)–N(1)	1.169(8)	1.163(7)
N(1)–C(49)	1.404(8)	1.410(8)
(b) Bond angle		
Cl(1)–Mo–P(1)	73.62(4)	75.86(4)
Cl(1)–Mo–P(2)	143.95(4)	146.89(4)
Cl(1)–Mo–P(3)	145.91(3)	143.76(3)
Cl(1)–Mo–P(4)	70.82(4)	72.16(4)
Cl(1)–Mo–C(47)	92.1(2)	88.0(2)
Cl(1)–Mo–C(48)	83.0(2)	85.4(2)
P(1)–Mo–P(2)	73.07(4)	72.98(4)
P(1)–Mo–P(3)	140.33(4)	138.93(4)
P(1)–Mo–P(4)	144.44(5)	146.13(5)
P(1)–Mo–C(47)	87.5(2)	87.9(2)
P(1)–Mo–C(48)	90.3(2)	87.4(2)
P(2)–Mo–P(3)	69.06(4)	69.23(4)
P(2)–Mo–P(4)	140.95(5)	134.43(5)
P(2)–Mo–C(47)	99.8(2)	101.7(2)
P(2)–Mo–C(48)	83.8(2)	82.3(2)
P(3)–Mo–P(4)	75.18(4)	74.77(5)
P(3)–Mo–C(47)	87.7(2)	84.5(2)
P(3)–Mo–C(48)	96.9(2)	102.7(2)
P(4)–Mo–C(47)	93.8(1)	101.7(1)
P(4)–Mo–C(48)	85.5(1)	79.3(1)
C(47)–Mo–C(48)	175.0(2)	172.6(2)
Mo–C(47)–O(1)	178.6(4)	178.7(5)
Mo–C(48)–N(1)	173.7(5)	174.4(5)
C(48)–N(1)–C(49)	177.0(5)	170.9(5)

of their poor quality, atom connecting scheme in **10b′** has been disclosed unequivocally as shown in Scheme 2. Thus, **10b** has a distorted pentagonal–bipyramidal structure with CO and Cl ligands at the axial positions and XyNC at one equatorial site. Probably because of the steric crowding of the pentagonal equatorial plane, one outer P atom P^4 is much deviated from the plane defined by other three P atoms and Mo, while the Xy ring is oriented almost perpendicularly to the equatorial plane. Replacement of the XyNC ligand at the *trans* site by the Cl anion, the ν(C≡O) band at 1872 cm^{-1} for **10a** shifts significantly to the lower frequency region (**10b**: 1844 cm^{-1}).

Among the related seven-coordinate Mo(II) complexes with four P ligands [10], a dicarbonyl complex with diphosphine ligands $[MoCl(CO)_2(Me_2PCH_2CH_2PMe_2)_2][PF_6]$ was fully characterized previously, which, by contrast, has a monocapped trigonal–prismatic geometry with two P–P–C basal planes together with the Cl ligand capping a P_4 face [11]. The structure of $[MoCl(CO)_2\{o\text{-}C_6H_4(AsMe_2)_2\}_2][I_3]$ [12] was also crystallographically determined to be monocapped trigonal–prismatic, while that of $[MoCl(CO)_2\{(i\text{-}Pr)_2PCH_2CH_2P(i\text{-}Pr)_2\}_2]Cl$ was presumed to be monocapped octahedral [13].

3. Experimental

3.1. General

All manipulations were carried out under N_2 using standard Schlenk techniques. Solvents were dried by common methods and distilled under N_2 before use. Complex **2** was prepared according to the method described previously [4], while other chemicals were obtained commercially and used as received.

NMR spectra were recorded on a JEOL alpha-400 spectrometer, while IR spectra were obtained by a JASCO FT/IR-420 spectrometer. For the ^1H NMR data below, those due to the **P4** ligand, aryl protons, and the solvating CH_2Cl_2 molecules are omitted. Numbering schemes for the P atoms are shown in Schemes 1 and 2. Elemental analyses were done with a Perkin–Elmer 2400 series II CHN analyzer.

3.2. Preparation of *4*

(1) A mixture of **2** (86 mg, 0.097 mmol) and PhC≡CH (22 μL, 0.20 mmol) in benzene (10 cm^3) was stirred at room temperature for 72 h. The resulting green solution was filtered and concentrated in vacuo. Addition of hexane afforded **4a** as green powder (45 mg, 47% yield). ^1H NMR (C_6D_6): δ 11.38 (dt, J(H–P) = 16.4, 4.0 Hz, 1H, HC≡). $^{31}P\{^1H\}$ NMR (C_6D_6): −10.4 (d, 1P, P^1), 41.0 (d, 1P, P^4), 56.3 (dd, 1P, P^2), 95.1 (s, 1P, P^3); $J(P^1–P^2) = 38$, $J(P^2–P^4) = 161$ Hz. Anal. Calc. for $C_{54}H_{48}Cl_2MoP_4$: C, 65.67; H, 4.90. Found: C, 65.24; H, 5.07%.

(2) Similar reaction carried out in CH_2Cl_2 (7 cm^3) afforded **4b** · $0.5CH_2Cl_2$ as a green solid (56 mg, 59% yield) after deposition from CH_2Cl_2-hexane. ^1H NMR ($CDCl_3$): δ 12.37 (tt, J(H–P) = 10.0, 1.6 Hz, 1H, HC≡). $^{31}P\{^1H\}$ NMR ($CDCl_3$): 55.1 (m, 2P, P^1 and P^4), 93.4 (m, 2P, P^2 and P^3). Anal. Calc. for $C_{54.5}H_{49}Cl_3MoP_4$: C, 63.54; H, 4.79. Found: C, 63.74; H, 4.89%. The NMR specra of **4a** and **4b** change reversibly upon replacement of the solvent from C_6D_6 to $CDCl_3$ and vice versa.

3.3. Preparation of *5*

(1) A mixture of **2** (96 mg, 0.11 mmol) and TolC≡CH (28 μL, 0.22 mmol) in toluene (10 cm^3) was stirred at 60 °C for 3 h. After cooling, the mixture was filtered and hexane was added to the concentrated filtrate, affording **5a** as green–brown solid (58 mg, 53% yield). ^1H NMR (C_6D_6): δ 11.37 (dt, J(H–P) = 14.0, 5.2 Hz, 1H, HC≡), 1.93 (s, 3H, Me).

$^{31}P\{^1H\}$ NMR (C_6D_6): −10.2 (d, 1P, P^1), 42.9 (d, 1P, P^4), 55.6 (dd, 1P, P^2), 97.2 (s, 1P, P^3); $J(P^1–P^2) = 40$, $J(P^2–P^4) = 162$ Hz. Anal. Calc. for $C_{55}H_{50}Cl_2MoP_4$: C, 65.95; H, 5.03. Found: C, 65.53; H, 5.11%.

(2) Reaction of **2** (102 mg, 0.115 mmol) and TolC≡CH (15 μL, 0.121 mmol) in CH_2Cl_2 (5 cm^3) at room temperature for 24 h afforded **5b** · $0.5CH_2Cl_2$ as green crystals after crystallization of the product from CH_2Cl_2-hexane (63 mg, 52% yield). ^1H NMR ($CDCl_3$): δ 12.14 (m, 1H, HC≡), 2.06 (s, 3H, Me). $^{31}P\{^1H\}$ NMR ($CDCl_3$): 55.7 (m, 2P, P^1 and P^4), 94.0 (m, 2P, P^2 and P^3). Anal. Calc. for $C_{55.5}H_{51}Cl_3MoP_4$: C, 63.84; H, 4.92. Found: C, 64.12; H, 4.99%.

3.4. Preparation of 6

(1) Reaction of **2** (68 mg, 0.071 mmol) and MeC≡CPh (29 μL, 0.23 mmol) in toluene (7 cm^3) at 60 °C for 12 h afforded a red–orange product solution. Crystallization of the product from toluene–hexane gave **6a** as yellow–brown crystalline solid (38 mg, 53% yield). ^1H NMR (C_6D_6): δ 1.60 (s, 3H, Me). $^{31}P\{^1H\}$ NMR (C_6D_6): −10.1 (m, 1P, P^1), 46.7–47.0 (m, 2P, P^4 and P^2), 93.8 (s, 1P, P^3). Anal. Calc. for $C_{55}H_{50}Cl_2MoP_4$: C, 65.95; H, 5.03. Found: C, 65.97; H, 5.25%.

(2) From the reaction of **2** (98 mg, 0.11 mmol) and MeC≡CPh (28 μL, 0.22 mmol) in CH_2Cl_2 (5 cm^3) at room temperature for 20 h, followed by crystallization from CH_2Cl_2-hexane, **6b** · $0.5CH_2Cl_2$ was obtained as a dark green solid (53 mg, 46% yield). ^1H NMR ($CDCl_3$): δ 1.79 (s, 3H, Me). $^{31}P\{^1H\}$ NMR ($CDCl_3$): 53.5 (m, 2P, P^1 and P^4), 93.1 (m, 2P, P^2 and P^3). Anal. Calc. for $C_{55.5}H_{51}Cl_3MoP_4$: C, 63.84; H, 4.92. Found: C, 63.26; H, 4.88%.

3.5. Preparation of 7

A mixture of **2** (92 mg, 0.10 mmol) and XyNC (14 mg, 0.11 mmol) in toluene (15 cm^3) was stirred at room temperature for 10 min. Addition of hexane to the resultant red–brown solution deposited an orange solid, which was filtered off, washed with ether, and then crystallized from CH_2Cl_2-hexane, yielding **7** as red crystals (53 mg, 50% yield). IR (KBr): 2026 ($\nu_{N\equiv C}$) cm^{-1}. ^1H NMR ($CDCl_3$): δ 1.89 (s, 6H, Me). $^{31}P\{^1H\}$ NMR ($CDCl_3$): 55.6 (ddd, 1P, P^1), 79.8 (ddd, 1P, P^4), 103.7 (ddd, 1P, P^2), 127.7 (ddd, 1P, P^3); $J(P^1–P^2) = 64$, $J(P^1–P^3) = 27$, $J(P^1–P^4) = 29$, $J(P^2–P^3) = 72$, $J(P^2–P^4) = 9$, $J(P^3–P^4) = 3$ Hz. Complex **7** dissolved in C_6D_6 showed the analogous NMR spectra. Anal. Calc. for $C_{55}H_{51}Cl_2MoNP_4$: C, 64.97; H, 5.06; N, 1.38. Found: C, 65.11; H, 5.18; N, 1.27%.

3.6. Preparation of 8

(1) A mixture of **2** (93 mg, 0.10 mmol) and XyNC (41 mg, 0.31 mmol) in toluene (15 cm^3) was stirred at room temperature for 1 h to give an orange suspension. The reaction mixture was filtered off, and the remaining solid was washed with ether and then crystallized from CH_2Cl_2-hexane, yielding **8** as a red crystalline solid (67 mg, 56% yield).

(2) Reaction of **2** (93 mg, 0.10 mmol) and XyNC (41 mg, 0.31 mmol) in CH_2Cl_2 (6 cm^3) afforded rapidly an orange solution. After 15 min, ether was added to a concentrated product solution, giving **8** as a red crystalline solid (70 mg, 61% yield). IR (KBr): 2057sh, 1989 ($\nu_{N\equiv C}$) cm^{-1}. ^1H NMR ($CDCl_3$): δ 1.06, 1.65 (s, 6H each, Me). $^{31}P\{^1H\}$ NMR ($CDCl_3$): 61.8 (m, 2P, P^1 and P^4), 93.6 (m, 2P, P^2 and P^3). Anal. Calc. for $C_{64}H_{60}Cl_2MoN_2P_4$ requires C, 66.96; H, 5.27; N, 2.44. Found: C, 67.30; H, 5.52; N, 2.14%.

3.7. Preparation of 8′

A mixture of **8** (34 mg, 0.030 mmol) and KPF_6 (17 mg, 0.092 mmol) in CH_2Cl_2 (7 cm^3) was stirred at room temperature for 24 h and then filtered. Addition of ether to the concentrated filtrate afforded **8′** · $0.5CH_2Cl_2$ (23 mg, 60% yield). Anal. Calc. for $C_{64.5}H_{61}Cl_2F_6MoN_2P_5$: C, 59.60; H, 4.73; N, 2.16. Found: C, 60.38; H, 4.72; N, 2.06%. Single crystals for X-ray diffraction were grown from $ClCH_2CH_2Cl$-ether.

3.8. Preparation of 9

A solution of **2** (115 mg, 0.130 mmol) in CH_2Cl_2 (10 cm^3) was stirred under a CO atmosphere for 1 h at room temperature. Addition of hexane to the concentrated product solution afforded **9** · $0.5CH_2Cl_2$ as a red–brown solid (72 mg, 58% yield). The reaction conducted in toluene also afforded **9** in comparable isolated yield. IR (KBr): 1793 ($\nu_{C\equiv O}$) cm^{-1}. $^{31}P\{^1H\}$ NMR ($CDCl_3$): δ 59.9 (m, 2P, P^1 and P^4), 96.0 (m, 2P, P^2 and P^3). Complex **9** dissolved in C_6D_6 showed the analogous NMR spectra. Anal. Calc. for $C_{47.5}H_{43}Cl_3MoOP_4$: C, 59.67; H, 4.53. Found: C, 59.74; H, 4.74%. Single crystals for X-ray diffraction were grown from CH_2Cl_2–C_6H_6–hexane.

3.9. Preparation of 10

(1) A mixture of **9** (51 mg, 0.056 mmol) and XyNC (15 mg, 0.11 mmol) in CH_2Cl_2 (10 cm^3) was stirred at room temperature for 20 h. Addition of ether to a concentrated product solution afforded **10a** · $0.5CH_2Cl_2$ as an yellow–brown solid (34 mg, 55% yield). IR (KBr): 2089 ($\nu_{N\equiv C}$), 1872 ($\nu_{C\equiv O}$) cm^{-1}. ^1H NMR ($CDCl_3$): δ 0.86 (s, 6H, Me). $^{31}P\{^1H\}$ NMR ($CDCl_3$): 61.1 (m, 2P, P^1 and P^4), 90.7 (m,

2P, P^2 and P^3). Anal. Calc. for $C_{56.5}H_{52}Cl_3MoNOP_4$: C, 62.42; H, 4.82; N, 1.29. Found: C, 63.02; H, 4.67; N, 1.31%.

(2) A mixture of **7** (36 mg, 0.035 mmol) in CH_2Cl_2 (5 cm^3) was stirred under CO for 90 min. Addition of ether to a concentrated product solution gave a mixture of **10a** · $0.5CH_2Cl_2$ and **10b** · $0.5CH_2Cl_2$ as an yellow–brown solid (21 mg, 54% yield). The ratio of **10a** and **10b** in the reaction mixture was 4:5 from the NMR criteria. **10b** · $0.5CH_2Cl_2$: IR (KBr): 2050 ($\nu_{N\equiv C}$), 1844 ($\nu_{C\equiv O}$) cm^{-1}. ^1H NMR ($CDCl_3$): δ 1.58 (s, 6H, Me). $^{31}P\{^1H\}$ NMR ($CDCl_3$): 75.6 (m, 2P, P^1 and P^4), 92.7 (m, 2P, P^2 and P^3). For a mixture of **10a** · $0.5CH_2Cl_2$ and **10b** · $0.5CH_2Cl_2$: Anal. Calc. for $C_{56.5}H_{52}Cl_3MoNOP_4$: C, 62.42; H, 4.82; N, 1.29. Found: C, 62.26; H, 4.94; N, 1.10%.

(3) A mixture of **10a** (30 mg, 0.029 mmol) and KPF_6 (17 mg, 0.092 mmol) in CH_2Cl_2 (6 cm^3) was stirred at room temperature for 24 h and then filtered. Addition of ether to the concentrated filtrate afforded **10a′** (23 mg, 69% yield). The X-ray analysis was carried out by using the crystals **10a′** · $1.5CH_2Cl_2$ present in this mixture without separation from the mother liquor.

(4) A solution of **10a′** (15 mg) in $ClCH_2CH_2Cl$ (6 cm^3) was heated to reflux for 2 h and the resultant mixture was dried up. Crystallization of the residue from CH_2Cl_2-hexane gave crystals of **10b′** (10 mg). The ^1H NMR spectrum of this crystals after drying in vacuo suggested the presence of 0.8 equiv of solvating CH_2Cl_2 molecule. **10b′** · $0.8CH_2Cl_2$: Anal. Calc. for $C_{56.8}H_{52.6}Cl_{2.6}F_6MoNOP_5$: C, 55.82; H, 4.34; N, 1.15. Found: C, 55.69; H, 4.47; N, 1.08%. Preliminary X-ray analysis was conducted by using the crystal **10b′** · $3CH_2Cl_2$ deposited from the reaction mixture, which was mounted without separation from the mother liquor.

3.10. X-ray crystallography

A single crystal of **7** was sealed in a glass capillary under argon, while those of **8′** · $1.7\,C_2H_4Cl_2$ · $0.3(C_2H_5)_2O$ and **9** · $1.15C_6H_6$ · $0.3C_6H_{14}$ · $0.12CH_2Cl_2$ were sealed in glass capillaries together with the mother liquor of crystallization. On the other hand, the crystals of **10a′** · $1.5CH_2Cl_2$ and **10b′** · $3CH_2Cl_2$ were mounted on cryoloops with mother liquor mixed with Paratone oil. Diffraction studies were done by a Rigaku AFC7R four-circle diffractometer for **7** or a Mercury-CCD diffractometer for others, equipped with a graphite-monochromatized Mo Kα source at 20 °C for **7**, **8′** and **9** or −160 °C for **10a′** and **10b′**. Details are listed in Table 5 except for those of **10b′**, for which only the preliminary results were available due to the poor quality of the crystals. For **10b′** · $3CH_2Cl_2$, formula: $C_{59}H_{57}Cl_7F_6MoNOP_5$, fw: 1409.08, space group: $P2_1/n$ (no. 14), a: 20.45(1), b: 11.455(6), c: 25.88(1) Å, β: 93.530(3)°, V: 6052(5) $Å^3$, Z: 4, $R_1 = 0.0805$ for 4531 reflections of $I > 2\sigma(I)$; $wR_2 = 0.246$ for 13 811 observed reflections.

Data collection were performed by using the WinAFC (for **7**) or CrystalClear (for others) program package [14].

Table 5
Crystal data for **7**, **8′**, **9**, and **10a′**

	7	**8′** · $1.7C_2H_4Cl_2$ · $0.3(C_2H_5)_2O$	**9** · $1.15C_6H_6$ · $0.3C_6H_{14}$ · $0.12CH_2Cl_2$	**10a′** · $1.5CH_2Cl_2$
Formula	$C_{55}H_{51}Cl_2MoNP_4$	$C_{68.6}H_{69.8}Cl_{4.4}F_6MoN_2O_{0.3}P_5$	$C_{55.8}H_{53.32}Cl_{2.24}MoOP_4$	$C_{57.5}H_{54}Cl_4F_6MoNOP_5$
Fw	1016.74	1447.91	1039.20	1281.68
Space group	$P2_1/c$ (No. 14)	$P2_12_12_1$ (No. 19)	$P\bar{1}$ (No. 2)	$P2_1/n$ (No. 14)
a (Å)	16.351(4)	11.724(1)	18.941(2)	20.878(5)
b (Å)	11.152(6)	22.116(2)	22.005(1)	25.347(6)
c (Å)	27.658(4)	26.634(3)	22.280(2)	23.361(6)
α (°)	90	90	61.509(3)	90
β (°)	105.05(1)	90	80.630(4)	110.819(1)
γ (°)	90	90	76.313(4)	90
V ($Å^3$)	4870(3)	6906(1)	7916(1)	11555(5)
Z	4	4	6	8
ρ_{calc} (g cm^{-3})	1.387	1.393	1.308	1.473
Crystal size (mm^3)	0.40 × 0.15 × 0.10	0.40 × 0.15 × 0.05	0.40 × 0.35 × 0.15	0.40 × 0.30 × 0.05
Number of unique reflections	11 173	15 778	36 102	26 381
Number of data with $I > 2\sigma(I)$	4807	8018	22442	11233
Number of variables	619	841	1766	1553
Transmission factor	0.841–0.947	0.730–0.974	0.751–0.925	0.824–0.970
R_1[a]	0.0610	0.0558	0.0529	0.0624
wR[b] or wR_2[c]	0.0686[b]	0.154[c]	0.150[c]	0.185[c]
GOF[d,e]	1.048[d]	1.008[e]	1.034[e]	1.004[e]

[a] $R_1 = \sum||F_o| - |F_c||/\sum|F_o|$ ($I > 2\sigma(I)$).
[b] $wR = \sum|w(|F_o| - |F_c||)/\sum w|F_o|$.
[c] $wR_2 = [\sum(w(F_o^2 - F_c^2)^2)/\sum w(F_o^2)^2]^{1/2}$ ($I > 2\sigma(I)$).
[d] GOF $= \sum|w(|F_o| - |F_c||)/\{$(no. observed) − (no. variables)$\}$.
[e] GOF $= [\sum w(|F_o| - |F_c|)^2/\{$(no. observed) − (no. variables)$\}]^{1/2}$.

All data were corrected for Lorentz and polarization effects as well as absorption (ψ-scans for **7** and multi-scans for others).

Structure solution and refinements were conducted by using the Crystal Structure program package [15]. The positions of non-hydrogen atoms were determined by Patterson methods (PATTY) [16] and subsequent Fourier synthesis (DIRDIF99) [17], which were refined with anisotropic thermal parameters by full-matrix least-squares techniques. Hydrogen atoms were placed at the calculated positions and included at the final stages of the refinements with fixed parameters.

Supplementary material

CCDC 659213, 659214, 659215 and 659216 contain the supplementary crystallographic data for **7**, **8′**, **9** and **10a′**. These data can be obtained free of charge from The Cambridge Crystallographic Data Centre via www.ccdc.cam.ac.uk/data_request/cif.

Acknowledgements

This work was supported by Grant-in-Aid for Scientific Research on Priority Areas (No. 18065005, "Chemistry of Concerto Catalysis") from the Ministry of Education, Culture, Sports, Science and Technology, Japan and by CREST of JST (Japan Science and Technology Agency).

References

[1] (a) C. Arita, H. Seino, Y. Mizobe, M. Hidai, Chem. Lett. 28 (1999) 611;
(b) C. Arita, H. Seino, Y. Mizobe, M. Hidai, Bull. Chem. Soc. Jpn. 74 (2001) 561.
[2] H. Seino, C. Arita, M. Hidai, Y. Mizobe, J. Organomet. Chem. 658 (2002) 106.
[3] T. Ohnishi, H. Seino, M. Hidai, Y. Mizobe, J. Organomet. Chem. 690 (2005) 1140.
[4] H. Seino, D. Watanabe, T. Ohnishi, C. Arita, Y. Mizobe, Inorg. Chem. 46 (2007) 4784.
[5] D. Watanabe, S. Gondo, H. Seino, Y. Mizobe, Organometallics 26 (2007) 4909.
[6] F. Niikura, H. Seino, Y. Mizobe, unpublished results.
[7] R. Ellis, R.A. Henderson, A. Hills, D.L. Hughes, J. Organomet. Chem. 333 (1987) C6.
[8] Y. Wang, J.J.R. Fraústo Da Silva, A.J.L. Pombeiro, M.A. Pellinghelli, A. Tiripicchio, R.A. Henderson, R.L. Richards, J. Chem. Soc., Dalton Trans. 1183 (1995).
[9] H. Seino, D. Nonokawa, G. Nakamura, Y. Mizobe, M. Hidai, Organometallics 19 (2000) 2002.
[10] (a) M.G.B. Drew, Prog. Inorg. Chem. 23 (1977) 67;
(b) M. Melnik, P. Sharrock, Coord. Chem. Rev. 65 (1985) 49.
[11] L.K. Fong, J.R. Fox, B.M. Foxman, N.J. Cooper, Inorg. Chem. 25 (1986) 1880.
[12] M.G.B. Drew, J.D. Wilkins, J. Chem. Soc., Dalton Trans. 2664 (1973).
[13] M. Jiménez-Tenorio, M.C. Puerta, P. Valerga, D.L. Hughes, J. Chem. Soc., Dalton Trans. 2431 (1994).
[14] CrystalClear 1.3.5: Rigaku Corporation, 1999. CrystalClear Software User's Guide, Molecular Structure Corporation, 2000: J.W. Pflugrath, Acta Crystallogr. D 55 (1999) 1718.
[15] CrystalStructure 3.8: Crystal Structure Analysis Package, Rigaku and Rigaku/MSC, 2000–2002. CRYSTALS Issue 10: D.J. Watkin, C.K. Prout, J.R. Carruthers, P.W. Betteridge, Chemical Crystallography Laboratory: Oxford, UK.
[16] PATTY: P.T. Beurskens, G. Admiraal, G. Beurskens, W.P. Bosman, S. Garcia-Granda, R.O. Gould, J.M.M. Smits, C. Smykall, The DIRDIF program system; Technical Report of the Crystallography Laboratory: University of Nijmegen, Nijmegen, The Netherlands, 1992.
[17] DIRDIF99: P.T. Beurskens, G. Admiraal, G. Beurskens, W.P. Bosman, R. de Gelder, R. Israel, J.M.M. Smits, The DIRDIF99 program system; Technical Report of the Crystallography Laboratory: University of Nijmegen, Nijmegen, The Netherlands, 1999.